Improving the atmospheric dispersion forecasts over Washington, D.C. using UrbanNet observations: A study with HYSPLIT model

Nebila Lichiheb*[1,2], Fong Ngan[3,4], and Mark Cohen[3]

[1] National Oceanic and Atmospheric Administration (NOAA), Air Resources Laboratory, Oak Ridge, TN 37830, USA.
[2] Oak Ridge Associated Universities, Oak Ridge, TN 37830, USA.
[3] National Oceanic and Atmospheric Administration (NOAA), Air Resources Laboratory, 5830 University Research Court, College Park, MD 20740, USA.
[4] Cooperative Institute for Satellites Earth System Studies, University of Maryland, 5830 University Research Court, College Park, MD 20740, USA.

Corresponding author*: Nebila Lichiheb
Email: nebila.lichiheb@noaa.gov

Abstract

UrbanNet data have been used to enhance the predictions of the Weather Research and Forecasting (WRF) model through observational nudging to improve temperature and wind predictions. HYSPLIT was utilized to understand the impact of using the observationally nudged WRF fields in dispersion modeling. The meteorological observations collected from the National Weather Service monitoring stations located at two major airports in Washington metropolitan area were also assimilated into WRF modeling. The results showed that observational nudging successfully adjusted WRF wind fields towards the observations and significantly reduced the forecast temperature bias at nighttime. The comparison of HYSPLIT simulations with and without the enhancement of the WRF model using UrbanNet and airport data showed significant differences in the pattern and direction of the dispersion plume especially during the early morning hours. Furthermore, ingesting the data from the closer airport to the downtown area in WRF provided HYSPLIT simulations very similar to the ones using UrbanNet data. This provides strong evidence that local data are essential to adjust weather prediction models routinely used to drive dispersion models. There was also evidence of increased mixing height when using local data collected in the downtown, mainly resulting from the increased surface heating in the city.

Key words: UrbanNet, Washington, D.C, Dispersion, WRF model, HYSPLIT model.

1. Introduction

Urban air pollution is one of the major issues related to the increase of the urban population (Fenger, 1999). The considerable increase in industrialization and traffic have been associated with elevated hazardous material releases and greenhouse gas emissions (Kelly and Fussell, 2015; Pataki et al., 2007). Atmospheric dispersion and deposition of hazardous materials in urban areas are therefore increasingly under investigation due to the potential impact on human health and the environment. In response to health and safety concerns, several dispersion models have been developed to analyze and predict the transport and dispersion of hazardous contaminants. Dispersion modeling in urban areas is based on various approaches such as Gaussian, Lagrangian and Eulerian models (et al., 2014). These modeling tools are mainly used in direct mode to provide real time predictions after an accidental or routine release at a known location (Onodera et al., 2021), or in inverse mode to identify the location of the source of a toxic release (Rudd et al., 2012; Chai et al., 2015). The primary objective of these model tools and their application types is to protect the urban population from accidental or intentional toxic releases. For emergency response applications, numerical predictions should be fast and accurate. In response to the urgent requirements from the atmospheric research community to provide an operational tool to predict the dispersion of hazardous contaminants in the atmosphere, the National Oceanic and Atmospheric Administration, Air Resources Laboratory (NOAA, ARL) developed the HYSPLIT transport and dispersion model (Draxler and Hess, 1997). It is a Lagrangian particle/puff model used by NOAA, other federal agencies, municipalities, and universities to run complex atmospheric transport and dispersion simulations needed for practical emergency response and other assessment applications (Stein et al., 2015).

Dispersion models (e.g. HYSPLIT) usually rely on meteorological information obtained from Numerical Weather Prediction (NWP) models (Benjamin et al., 2019), such as the Weather Research and Forecasting (WRF) model (Powers et al. 2017). The gridded data fields output from these meteorological models are usually interpolated to a variety of different vertical coordinate systems prior to outputs (Draxler and Hess, 1998). These interpolations remain a topic of considerable uncertainty (Ngan et al., 2015a), especially for complex environments such as urban areas. Furthermore, NWP models generally have very limited information about the changes in surface roughness associated with street canyons and buildings, which cause an increase in turbulent mixing and a slowing of the local flow within the urban core (Britter and Hanna, 2003). hese models are also typically based on classical micrometeorological data gathered tens of kilometers away from the urban area in question and sufficiently above the surface roughness layer (Hicks, 2005). In urban area, the surface roughness layer is of special interest because it is within this layer that people live and work and where they are most susceptible to exposure to atmospheric contaminants (Hicks et al., 2013). Due to this complexity, meteorological models for the urban environment are still under development (Baklanov et al., 2018).

In order to provide more accurate meteorological inputs to operational dispersion models in urban areas, there is a need to combine NWP model simulations and local meteorological observations (Haupt et al., 2019). The latter are rarely available in urban areas. In recognition of this flaw, a research program called DCNet was established in 2003 by the NOAA ARL and is recently evolving into an ongoing UrbanNet project to collect micrometeorological information at multiple sites across the Washington, DC, area. In terms of making best use of existing data to improve dispersion model predictions for urban and city applications, the UrbanNet data provide a unique opportunity for real-time meteorological observations over the greater National Capital Region (NCR) to support development of numerical weather prediction models as well as provide the meteorological observations for improved NWP outputs to drive dispersion models for emergency application (Hicks et al., 2012). The NCR was selected as the focal area, mainly because building heights in Washington, D.C are constrained by law, they are therefore fairly homogeneous. In conjunction with the relative simplicity of the terrain, this represents a useful initial environment for improving the description of dispersion in the urban roughness layer where people might be exposed.

The main goal of this study is to investigate the inclusion of local observations to adjust numerical weather predictions and its impact on conventional dispersion modeling in urban areas. Lichiheb et al. 2023 evaluated the forecast outputs of the North American Mesoscale (NAM) model with UrbanNet measurements for three years. The results in Washington, D.C. showed that NAM wind speed predictions tend to be highest in light and high wind conditions and the direction of the predicted plume needs to be adjusted by subtracting 20 degrees if NAM data is used in the circumstances of Washington, D.C. In this context, a data assimilation method is needed to establish more realistic flow conditions based on local observations. The meteorological observations collected from the UrbanNet network may be used directly to drive HYSPLIT simulations after converting the data to the HYSPLIT meteorological input file format. However, the tower observation at one location only represents a limited area spatially and is not sufficient to reveal the horizontal and vertical structure of the boundary layer (Ngan et al. 2023). Using a single observation site may not provide realistic flow conditions to drive a dispersion simulation especially during nighttime and the morning transition hours of the planetary boundary layer (PBL). For this reason, the Four-dimensional data assimilation (FDDA; so-called *nudging*) is a better approach. The FDDA is a well-known and efficient method in WRF to reduce model bias by incorporating observations during the simulation (Deng et al. 2009). This approach considers gridded analysis fields (analysis nudging) or individual observations (observational nudging) and corrects biases for temperature, moisture, and u- and v-components of wind at each integration time step (Ngan et al., 2015b). The nudging tool in WRF has been widely used and has been demonstrated to be beneficial in generating improved meteorological input data for dispersion modeling (Onodera et al., 2021, Hegarty et al. 2013, Ngan et al., 2023, Ngan et al. 2015b, Tomasi et al. 2019, Jia et al. 2021, Abida et al. 2022).

In this study, UrbanNet observations at the U.S. Department of Commerce Herbert C. Hoover Building (HCHB) station have been used to enhance the predictions of the WRF meteorological model through observational nudging to improve temperature and wind predictions. The HYSPLIT dispersion model was used to illustrate the impact of ingesting the observational nudged WRF fields in dispersion modeling. In addition to the meteorological measurements obtained at the top of HCHB, another set of available observations was tested. The meteorological datasets collected from the National Weather Service (NWS) monitoring stations located at the regional major airports in Washington, DC were used in WRF simulations and the results were compared against the HCHB data. NWS station at Ronald Reagan National Airport (DCA) is located approximately 5 kilometers south of the HCHB complex. NWS station at Dulles International Airport (IAD) is located roughly 35 km northwest of the HCHB complex.

We selected a two-week period – Jan 12-19, 2017 and July 4-11, 2017 – to perform sensitivity tests on the nudging configurations. HYSPLIT simulations for a 3-hr hypothetical unit emission release were conducted using the nudged WRF model fields, and the results were compared with the simulation with non-nudged WRF. In the first part of the analysis, nudged WRF simulations using the HCHC data will be compared against the non-nudged WRF outputs and the HCHB observations. In the second part, HYSPLIT simulations will be conducted using non-nudged and nudged WRF fields. The results will then be compared to demonstrate the impact of local observations on the improvement of the prediction of hazardous material dispersion in a complex environment such as an urban area. A third part will present HYSPLIT results driven by nudged WRF using meteorological datasets collected from the DCA and IAD airports in order to test the existing capabilities. The results will then be compared against the HYSPLIT runs using non-nudged and nudged WRF using HCHB data to demonstrate the importance of collecting meteorological data in or close by the downtown area to improve the accuracy of dispersion modeling in downtown Washington, D.C.

2. Material and Methods

2.1. UrbanNet observations at the NCR: HCHB station

UrbanNet (formerly DCNet) is a meteorological network in Washington D.C. which collects standard meteorological data and also measures characteristics of atmospheric turbulence . The installation atop the U.S. Department of Commerce Herbert C. Hoover Building (HCHB) at 1401 Constitution Avenue, Northwest, Washington, DC (38.894°N, 77.033°W) represents the core monitoring station for UrbanNet network in the NCR. The HCHB station is the only currently active UrbanNet site, .

This UrbanNet station has served as the central point within the NCR with a building height of approximately 25 m above ground level (AGL), and has been unaffected by data interruptions caused by resource limitations. The HCHB station was installed in 2003 with data archiving starting in 2004. Measurements were made using a 10 m meteorological tower above the HCHB rooftop. The HCHB data are recorded at a rate of 10 Hz then reported as 15 min averages. More details on the description of instrumentation and data analysis associated with the HCHB are presented by Pendergrass et al. (2020). The representativeness of the HCHB dataset for the NCR has been analyzed by examining former sonic anemometer data derived during 2008 from 7 UrbanNet stations within the NCR. The comparison of the wind speed and standard deviation of wind direction data demonstrates the representativeness of the HCHB site measurements as described in Lichiheb et al., (2023).

In this study, we focused on the periods from January 12 to 19 and from July 4 to 11 of 2017 to understand the use of tower measurements in an urban environment in WRF to improve meteorological fields and related effects on transport and dispersion simulations. The selected data have been used here after quality assurance (QA) and quality control (QC) (Pendergrass et al., 2020).

2.2. Model description and configurations

a. Meteorological model: WRF

The WRF model (version 4.2.2) is configured for a domain with a horizontal grid spacing of 3 km (Figure 1). The projection center is at 38.9°N and 77.0°W, with standard latitude at 38.0°N. A total of 33 vertical layers were defined with a higher resolution near the surface and 100 hPa for the model top. There were 20 layers below 850 hPa (~1.5 km) with the mid-layer height of the first model layer at ~8 m. The simulations were initialized using GDAS data in 0.25-degree spatial resolution and available every 6 hours (https://rda.ucar.edu/datasets/ds083.3). The daily WRF runs had a 30-hr duration including a 6-hr spin-up period (i.e., starting at 18:00 UTC on the previous day). The WRF meteorological fields were output every 15 minutes. The physics options for the WRF simulations included the rapid radiative transfer model for radiation parameterization (RRTMG; Iacono et al. 2008), WSM6 for microphysics (Lim and Hong, 2010), the Grell 3D Ensemble for the sub-grid cloud scheme (Grell and Devenyi, 2002), the Noah land-surface model (Chen and Dudhia, 2001), the Monin-Obukhov surface scheme, and the Shin-Hong scheme for PBL parameterization (Shin and Hong, 2014).

The 15-minute HCHB data were converted to the format required by WRF's observational nudging. A similar conversion process was applied to the hourly DCA and IAD data to create nudging files for WRF simulations. The locations of the HCHB, DCA and IAD stations are shown in Figure 1. Three sets of WRF simulations were carried out without and with observational nudging using different observation datasets and nudging settings. The variables for observational nudging were temperature and the u- and v-wind components. Table 1 shows the observational nudging parameters that were used in WRF simulations to investigate the influence of the observational data. The overall weighting factors are obs_coef_wind and obs_coef_temp for wind and temperature, respectively. They determine the strength of the correction made to the model fields – stronger nudging coefficients produce more significantly adjusting the model value to the observed value. However, too strong observation nudging may prevent physical tendency terms in the model reaching a consistent solution. We follow the nudging coefficients used in Ngan et al. (2023) but increase obs_coef_wind in the run using HCHB observation. The temporal weighting, twindo, is the time window when applying observational nudging. We set it according to the temporal frequency of the observational data – 15 minutes and one hour for HCHB and DCA (also IAD), respectively. The vertical spreading indicates the influence of surface observation linearly decreases with height, with the full weighting at the surface and becoming to zero at 50 m AGL. The horizontal spreading depends on the radius of influence which is set to 20 km in this study (Figure 1).

1) Non-nudged: without observational nudging;
2) Nudged-35m: using HCHB 15-min data collected at 35 m above ground level for observational nudging;
3) Nudged-surface: using DCA or IAD hourly data collected at surface for observational nudging.

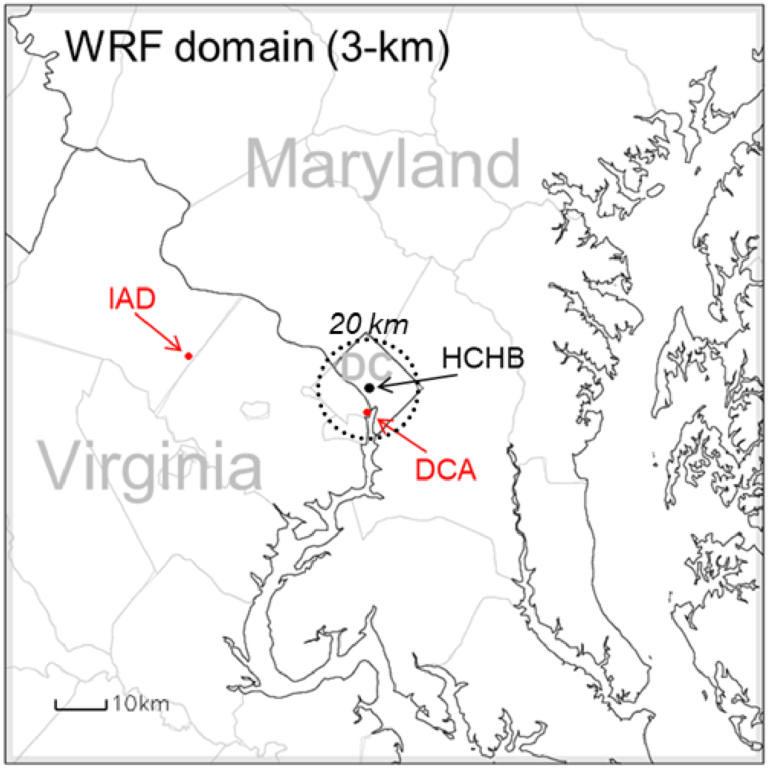

Figure 1: WRF modeling domain, HCHB location, and two NWS surface stations: DCA and IAD. Note that the circle indicates the 20 km radius of influence used for observational nudging.

Table 1: WRF observational nudging parameters used in this study.

	Observations	Half-period time window for using obs (twindo)	Nudging coefficient for wind (obs_coef_wind)	Nudging coefficient for temperature (obs_coef_t)	Horizontal radius of influence (rinxy)	Vertical spreading for u/v/t
Non-nudged	-	-	-	-	-	-
Nudged-35m	HCHB	15 minutes	6.4e-3 s-1	1.2e-3 s-1	20 km	-
Nudged-surface	DCA or IAD	1 hour	3.2e-3 s-1	1.2e-3 s-1	20 km	0 – 50 m

b. Dispersion model: HYSPLIT

HYSPLIT simulations for hypothetical releases were conducted using non-nudged and nudged WRF meteorological fields. The HYSPLIT model (version 5.2.1) is configured for a continuous release at the HCHB location at 20 m AGL with a total of 50,000 computational Lagrangian particles over 3 hours using a unit emission of 1 gram per hour. The concentrations were calculated on a 0.01 x 0.01 degrees (~1 x 1 km) horizontal grid using 30-minute temporal averaging. We used two vertical layer settings, 0 – 100 m and 0 – 1000 m, for the concentration calculation. HYSPLIT used planetary boundary layer height (PBLH) directly from WRF's prediction. The vertical mixing scheme utilized in HYSPLIT was the Kantha-Clayson method, which uses the friction velocity, boundary layer depth, and other state variables from WRF to compute the turbulent velocity variances for the dispersion calculation (Ngan et al. 2019).

3. Results and Discussion

3.1. Observational nudging analysis

In order to enhance the predictions of the WRF meteorological model, the 15 min HCHB data were ingested through observational nudging. At the HCHB station, a three-dimensional sonic anemometer system is installed on the top of a 10 m meteorological tower mounted above the HCHB rooftop. The building height is around 25 m AGL, thus the measurement height is approximately 35 m AGL. The placement of the HCHB observation in the meteorological simulation was determined according to the height of observation (i.e. 35 m AGL) and WRF's vertical layer. According to the model configuration used in this study, the 3rd WRF layer is ~ 44 m AGL (mid-layer height) and its thickness is 24 m.

Figure 2 shows the comparisons of observed and modeled wind speed, wind direction, and air temperature from 4-11 July, 2017. Note that the model wind and temperature are from the 3rd model layer which is the closest layer to the measurement height. This figure also includes the PBLH simulated by WRF model using the nudged and non-nudged scenarios without comparison to observations since no PBLH measurements were available at the HCHB station in 2017. This comparison shows that the nudged simulations provide results closer to the measurements. In fact, the observational nudging successfully adjusted the wind speed and wind direction toward the HCHB observations with significantly smaller mean absolute error (MAE) for the nudged WRF scenario compared to the non-nudged one (Table 2). For air temperature, both nudged and non-nudged WRF simulations are in good agreement with the HCHB observations during day time. However, nocturnal cold bias for temperature was present in the non-nudged simulation during the study period. Other studies, such as Branch et al. 2021, Chen et al. 2022, and Piersante et al. 2021, also reported WRF's underprediction of temperature at night. The observational nudging significantly reduces the temperature forecast bias at night time, leading to a significant impact on the PBLH during night time and at early morning transition hours, specifically on July 7th. Yet, the observational nudging slightly over-adjusted the temperature resulting in a small positive bias. It should also be noted that, on July 7th a significant inaccuracy in wind direction predictions is detected during the early morning when local observations are not used to correct biases. Relatively accurate wind predictions in the non-nudged run were simulated on other days, such as July 9th, and we do not notice a large difference between non-nudged and nudged wind fields.

Table 2: Summary of the statistical analysis results obtained by comparing the 15 min HCHB data against the non-nudged WRF outputs and the nudged WRF outputs at 35 m AGL from July 4-11, 2017.

	Mean Absolute Error (MAE)		
	T (°C)	WS (ms^{-1})	WD (deg)
Non-nudged WRF	1.403	1.166	27.815
Nudged-35m	1.016	0.853	18.048

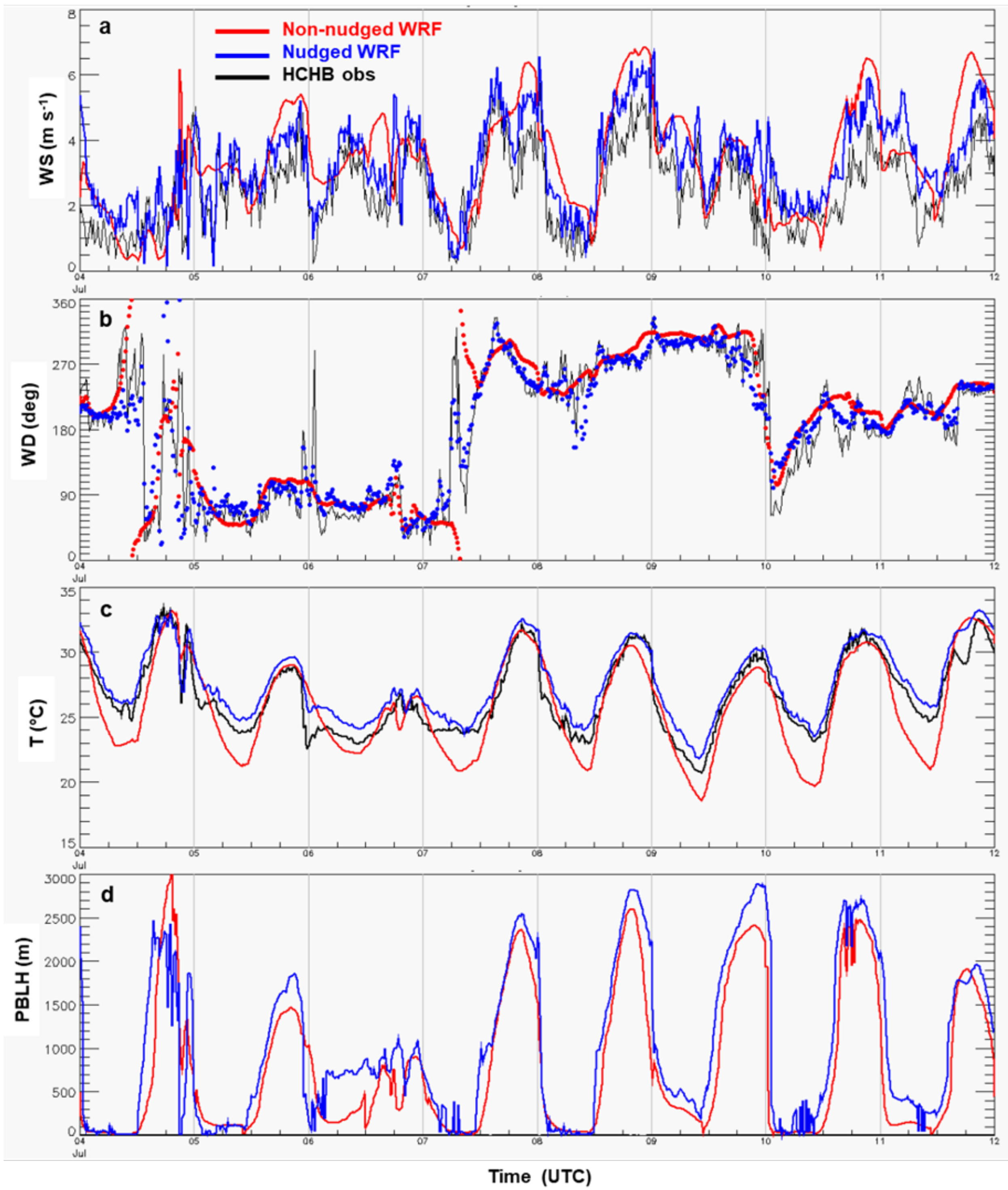

Figure 2: Time series of observed and simulated: (a) wind speed (WS), (b) wind direction (WD), (c) air temperature (T), and (d) PBLH. The planetary boundary layer height (PBLH) figure shows only WRF simulations.

3.2. Dispersion simulation analysis

In order to investigate the impact of using the observational nudged WRF fields detected on July 7 (Figure 2.b), HYSPLIT simulations were conducted during that day using non-nudged and nudged WRF for hypothetical releases. The simulations started at 05:00 UTC (01:00 EST), using a unit emission (1 gram per hour) with a total of 50,000 particles over 3 hours. Note that the concentration calculation counted for the particles in the volume of 1 x 1 km (0.01 x 0.01 degrees) horizontally in 10-minute temporal averaging. Figure 3 shows the concentration plots at 08:00 UTC (i.e., three hours after the initiation) from simulation using the non-nudged WRF (Figure3.a) and nudged WRF (Figure3.b) averaged over a vertical layer from 0 – 100 m AGL. Figure3.c is for the same simulation but with concentrations averaged over a layer 0 – 1000 m above ground (Figure3.c). HYSPLIT simulations using nudged WRF with vertical dimension of concentration grid of 100 m AGL (Figure3.b) shows a plume covering a small area compared to the HYSPLIT simulations using non-nudged WRF outputs (Figure3.a). The vertical distribution of particles presented in the bottom figures show that HYSPLIT simulations using non-nudged meteorological data kept the particles near the surface (< 100 m AGL), however HYSPLIT simulations using nudged WRF outputs induced a dispersion of particles to higher altitudes (> 1000 m AGL). In the model run using nudged WRF and vertical grid 0 – 1000 m AGL (Figure3.c), the dispersion plume went to a direction towards the north and north-east. The direction of the predicted plume using the non-nudged WRF simulation is significantly different (west and south-west direction) with different concentration levels. These results clearly demonstrate the need for local data to adjust weather prediction models routinely used to initialize dispersion models over urban areas on which critical decisions for emergency response are based. As discussed by Hicks (2005), predictions of plume dispersion made without local data can be completely misleading.

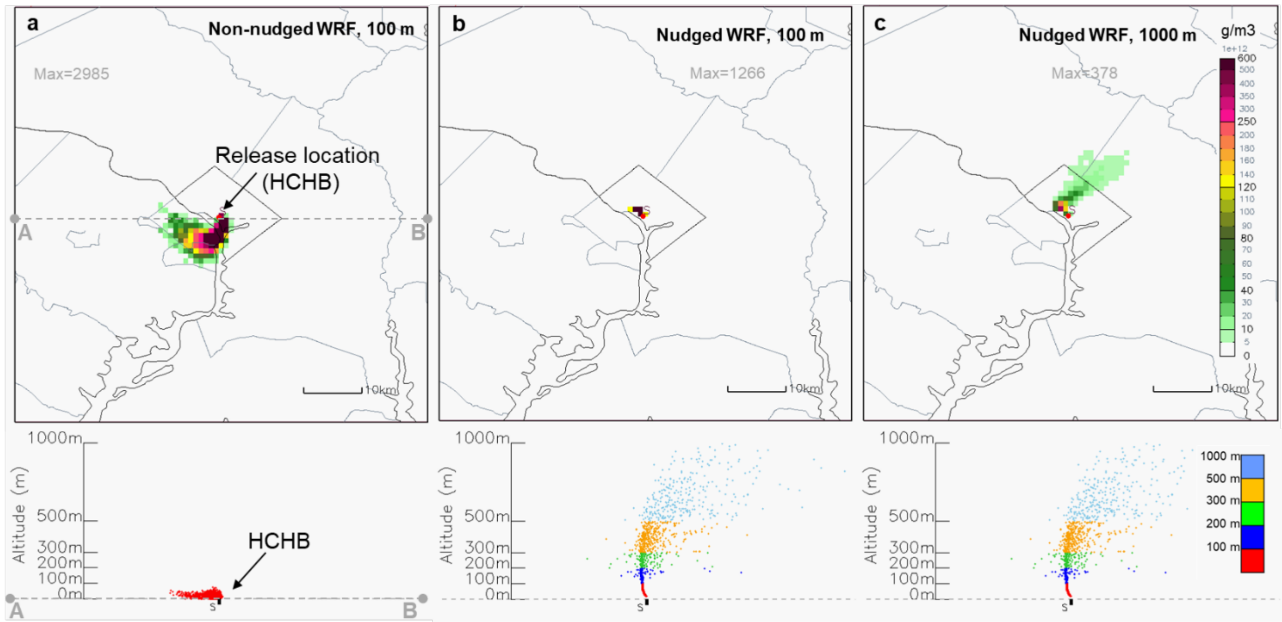

Figure 3: HYSPLIT simulations using (a) non-nudged WRF, (b) nudged WRF with concentrations averaged over 0-100 m AGL, and (c) nudged WRF with concentrations averaged over 0-1000 m AGL at 08:00 UTC on July 7, 2017 (for simulated hypothetical release of 1 g/hr starting at 05:00 UTC). The top figures show the horizontal distribution of tracer concentration and the bottom figures show the vertical distribution of the computational point particles used in the simulation.

To complete our analysis, we selected another day during the week from 4-11 July (July 9) when wind direction predictions are in agreement with the measurements without observational nudging (Figure 2.b). Similar HYSPLIT simulations were conducted on July 9 to study the impact of nudging the WRF model on the transport and mixing of pollutants. The results are shown in Figure4. The vertical distribution of particles presented in the bottom panel of Figure 4 shows that simulated particles using nudged WRF were mixed to a higher altitude (500 m and above), while the non-nudged meteorological data kept most of the particles below 100 m. HYSPLIT simulations using nudged WRF with a concentration averaging layer of 0-1000 m AGL (Figure4.c) shows similar horizontal patterns of plume movement compared to the dispersion plume simulated using the non-nudged WRF outputs with a direction towards the southeast. The similarity in the plume movement between the non-nudged and nudged scenarios may be explained by the good agreement between non-nudged WRF simulated and observed wind direction (Figure 2.b). Figure 4c also shows a narrower plume compared to the dispersion plume simulated using the non-nudged WRF outputs This result may be explained by the fact that simulated particles in the nudged scenario were dispersed to higher altitudes (where wind speed is stronger compared to the surface) and moved faster with a narrower plume compared to the non-nudged scenario.

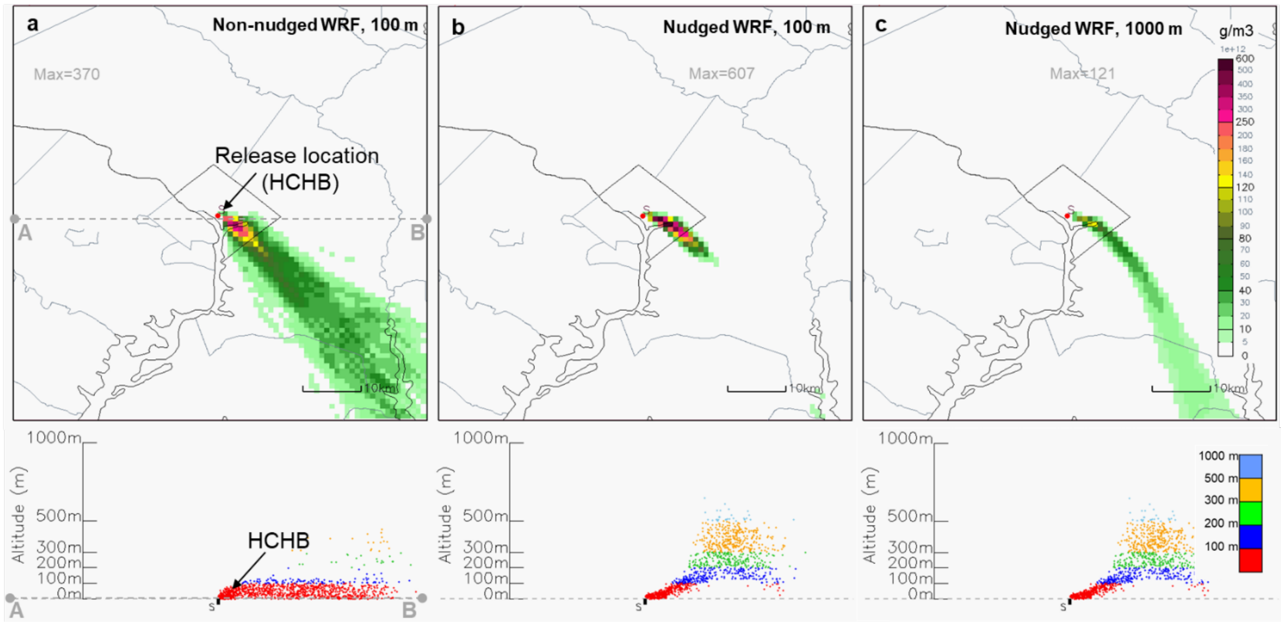

Figure 4: HYSPLIT simulations using (a) non-nudged WRF and (b) nudged WRF with concentrations averaged over 0-100 m AGL, and (c) nudged WRF with concentrations averaged over 0-1000 m AGL at 08:00 UTC on July 9, 2017 (starting at 05:00 UTC). The top figures show the horizontal plots of tracer concentration and the bottom figures show the vertical distribution of particles.

The comparison between HYSPLIT runs using non-nudged and nudged meteorological inputs shows a significant difference in the pattern and direction of the dispersion plume in the early morning hours when wind observations are not well simulated by non-nudged WRF (e.g. on July 7th). This result highlights the fact that the observational nudging successfully adjusted the predicted wind towards the measurements, and presumably, more accurate wind and temperature data should lead to a more accurate dispersion simulation. However, as shown from the July 9th case, there is evidence of increased mixing height when using local data from the HCHB station whether or not non-nudged WRF simulations are in agreement with the observations. Determining the mixing height is a key to understand and model the structure of the urban boundary layer where most of the world's population live and work (Barlow, 2014). HYSPLIT runs using non-nudged WRF were unable to detect the higher vertical transport and mixing mainly because WRF model cannot see the presence of urban-land cover like most of the NWP models. These models have, therefore, no information about the large surface roughness imposed by the different obstacles of the urban environment (buildings, streets, vegetation, etc) which impose an increased turbulence (Britter and Hanna, 2003). The enhanced vertical mixing may also be related to the increased surface heating in urban areas. Grimmond and Oke (1999) investigated the storage heat flux for seven urban areas within Canada, the United States, and Mexico and demonstrated that storage heat flux is greater in more urban cities. Piringer et al. (2007) conducted similar field experiments in several European cities. Their urban heat flux observations demonstrated a significant perturbation of the surface energy balance partitioning compared to rural areas, which drove the evolution and vertical structure of the urban boundary layer. In this context it's important to highlight that the measured heat flux at the HCHB station remains positive and rarely falls below zero even during night time (Pendergrass et al., 2020). These observations show that the near-surface layer seldom becomes stable due to the large releases of the heat generated from the city. This result is consistent with the HYSPLIT dispersion simulations when the HCHB data are ingested in WRF model.

To further investigate this aspect, cross-section figures of temperature and vertical velocity for July 7th (Figure 5) and July 9th (Figure 6) are provided from the non-nudged and nudged WRF simulations at 08:00 UTC (04:00 EST). On July 7, the nudged WRF run provided a higher temperature near the HCHB station from the surface to about 500 m AGL. This increased temperature has led to a significantly higher vertical velocity above and west of the HCHB site, as shown in Figure 5. A slightly higher temperature was simulated on July 9th at the HCHB site at the lower part of the boundary layer (from the surface to about 200 m, inducing higher vertical velocity above the HCHB station (Figure 6). These findings help to explain the enhanced vertical transport and mixing in the dispersion simulations using nudged WRF data (Figure 3 and 4). Beside the advantage of adjusting the primary meteorological variables (wind and temperature), the observational nudging using HCHB data allowed a better description of the urban PBL structure particularly in the early morning hours. Understanding the structure and behavior or the urban PBL is critical for modeling pollutant dispersion especially during the morning transition hours (Cuchiara and Rappengluck, 2019; Ngan et al., 2023).

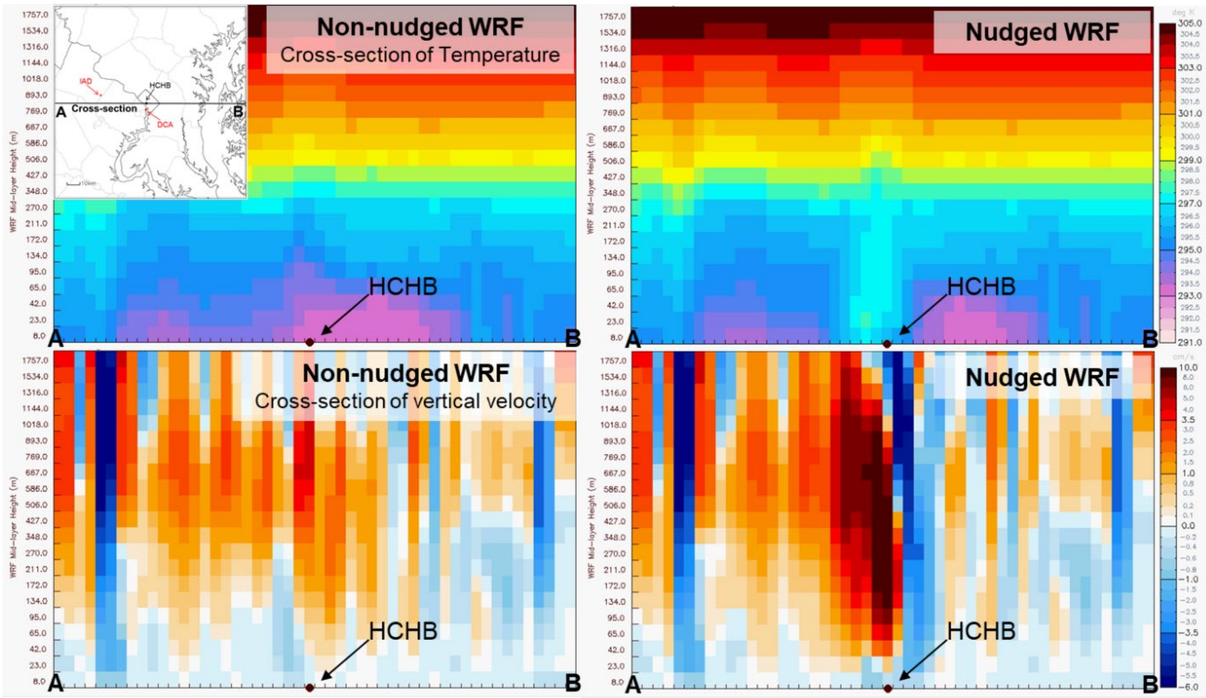

Figure 5: The cross-section (A-B on the map) of temperature (top) and vertical velocity (bottom) for non-nudged (left) and nudged WRF (right) at 08:00 UTC on July 7th

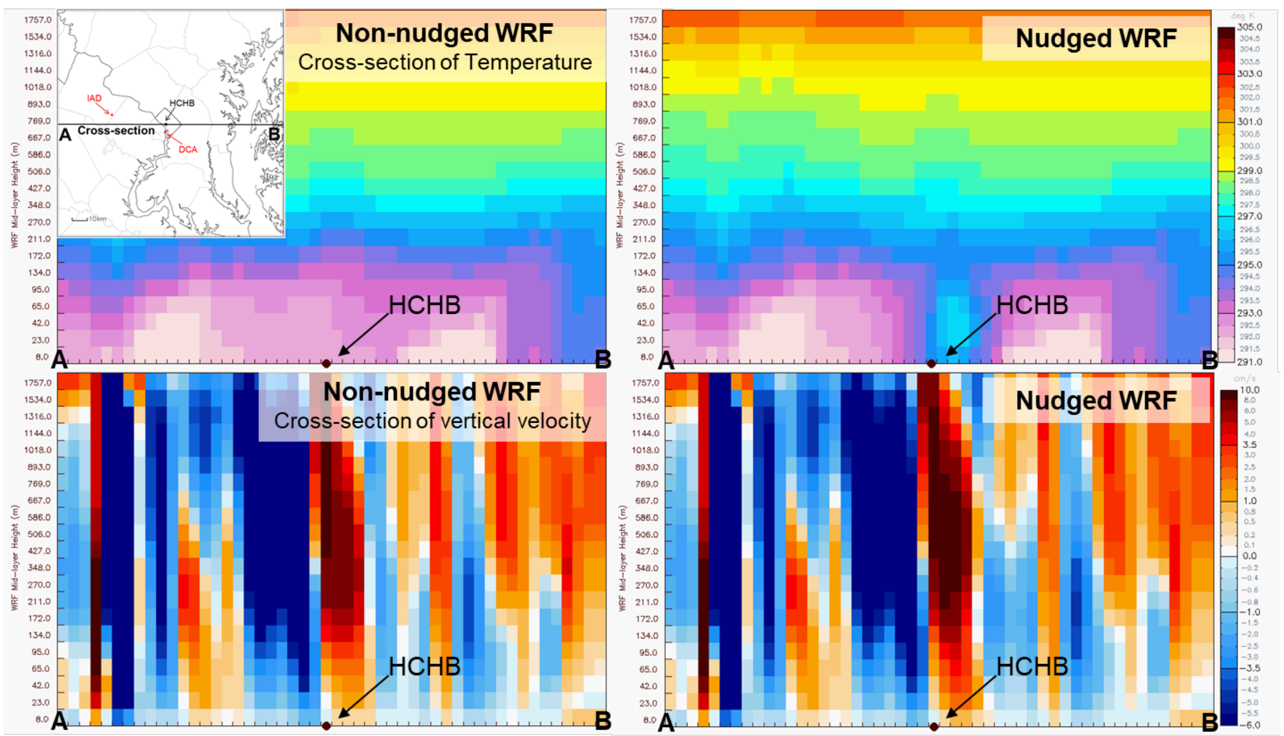

Figure 6: The cross-section (A-B on the map) of temperature (top) and vertical velocity (bottom) for non-nudged (left) and nudged WRF (right) at 08:00 UTC on July 9th

3.3. Comparison to NWS stations

Classical micrometeorological data are usually gathered from NWS monitoring stations located at major airports, often tens of kilometers away from urban areas where conditions are considerably different from downtown (Hicks, 2005). There are two major airports in the Washington, D.C. area: (i) Ronald Reagan National Airport (DCA), and (ii) Dulles International Airport (IAD). The DCA airport is located only a few kilometers from the downtown area. This section focuses on testing the existing data capabilities and analyzing the significance of routine local data to improve the predictions of hazardous material dispersion in the Washington, D.C. area. To this end, the hourly DCA and IAD surface data were ingested into the WRF model at the surface model layer from January 12 to 19, 2017. We then selected January 16 to conduct HYSPLIT simulations using non-nudged and nudged WRF (at the surface model layer) for hypothetical releases. We also carried out simulations with WRF nudged by HCHB data during this period. The simulations started at 05:00 UTC, using a unit emission (1 gram per hour) with a total of 50,000 particles over 3 hours. The concentration calculations were on a grid with horizontal spacing 1 x 1 km (0.01 x 0.01 degrees) for one vertical layer from 0 – 1000 m above ground. Figure 7 shows the concentration plots at 08:00 UTC (i.e., three hours after the initiation) for non-nudged WRF (Figure 7.a), nudged WRF using HCHB data (Figure 7.b; labeled as nudged HCHB), nudged WRF using DCA data (Figure 7.c; labeled as nudged DCA), and nudged WRF using IAD data (Figure7.d; labeled as nudged IAD). The HYSPLIT simulation using non-nudged WRF (Figure 7.a) shows a very similar pattern of plume movement to the simulated plume using IAD data (Figure 7.d), both with a direction towards the west-northwest. Furthermore, the vertical distribution of particles presented in the bottom panels of figures 8.a and 8.d show that HYSPLIT simulations using non-nudged and nudged WRF-IAD kept the particles near the surface (< 200 m AGL). The observation collected at IAD had no influence on the meteorological condition in downtown DC simulated by WRF. These results are significantly different compared to the HYSPLIT results driven by nudged WRF-HCHB. Figure 7.b shows that the observational nudging using HCHB data resulted in a wider plume moving to the north. Furthermore, the simulated particles were dispersed to higher altitudes (1000 m AGL). The direction of the predicted plume using nudged WRF-DCA is the west and north-west with simulated particles also mixed to a higher altitude (about 1000 m AGL). The similarity in the plume movement and particle distribution between the nudged WRF-HCHB and nudged WRF-DCA simulations demonstrate the importance of collecting meteorological data in or close by the downtown area to better describe all of the motions that are controlling local dispersion.

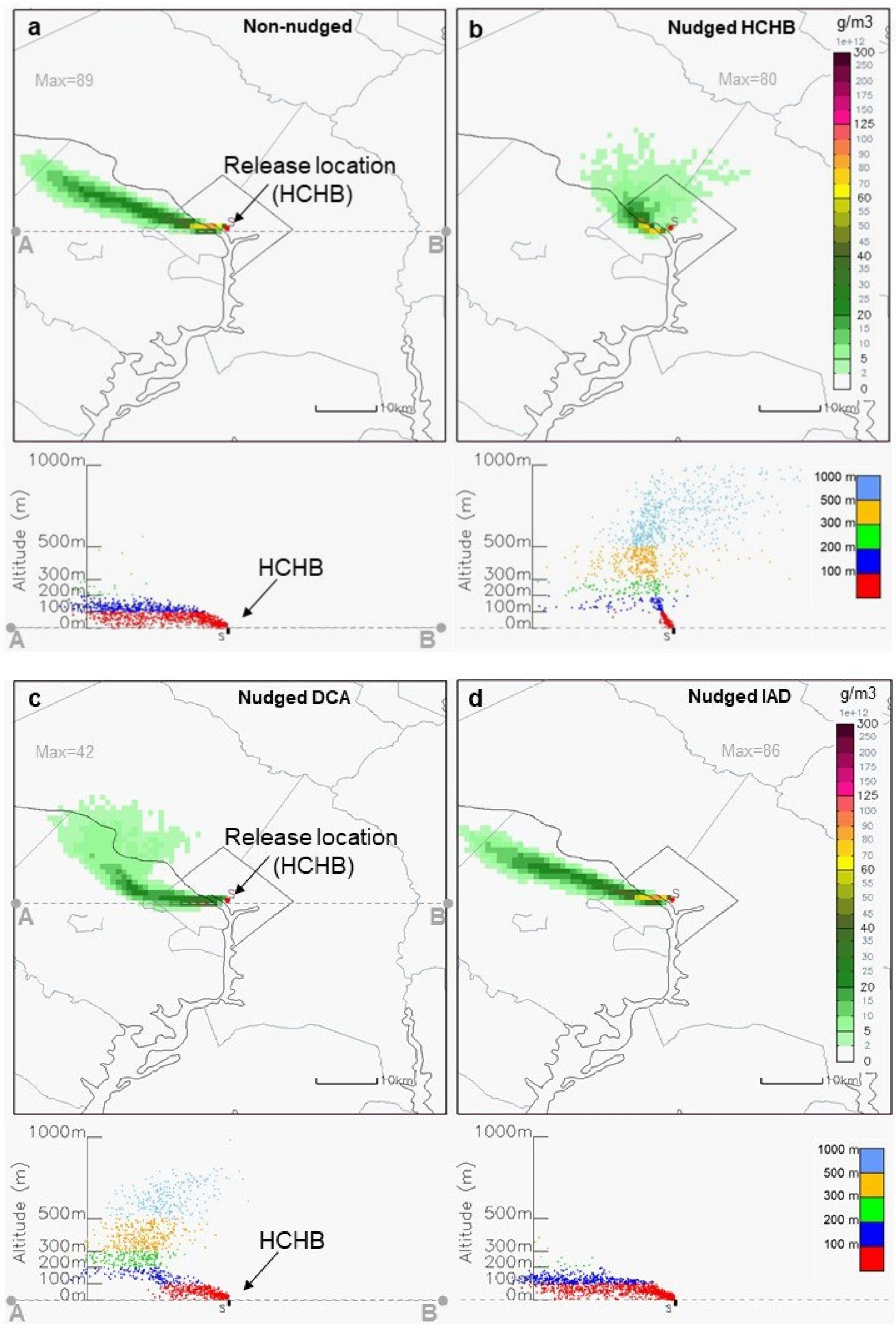

Figure7: HYSPLIT simulations using non-nudged WRF (a), nudged WRF using HCHB data (b), nudged WRF using DCA data (c) and nudged WRF using IAD data (d) at 08:00 UTC on January 16, 2017 (starting at 05:00 UTC). The top figures show the horizontal plots of tracer concentrations and the bottom figures show the vertical distribution of particles.

4. Conclusions

The UrbanNet (formerly DCNet) research program was established in the NCR in response to the 9/11 terrorist attacks to provide high-resolution meteorological measurements to improve the accuracy of weather forecast models and hence urban transport and dispersion models for emergency response. The network stations and sensors were intentionally arranged to report on the wind and temperature fields affecting the local population and to attempt to increase the accuracy of downwind impact forecasts. The central objective of this historical and current study is to assimilate local observations into NWP models to provide more accurate meteorological fields to drive operational air pollution models. In this context, HCHB data have been used to enhance the predictions of the WRF model through observational nudging. The results showed that the observational nudging successfully adjusted the wind data towards the HCHB observations and significantly reduced the temperature forecast bias at night time at this site.

HYSPLIT simulations using non-nudged versus nudged fields showed significant differences in the pattern and direction of the dispersion plume, particularly when wind observations are not well simulated by non-nudged WRF during the early morning hours. There was also evidence of increased mixing height when using local data from the HCHB station whether or not non-nudged WRF simulations agree with the observations. Indeed, HYSPLIT simulations utilizing non-nudged meteorological data kept the majority of the particles below 100 m AGL, however nudged WRF outputs induced dispersion of particles to higher altitude, surpassing 1000 m AGL. The mixing height is a critical and influential parameter for most air quality models, and is relatively uncertain. Enhanced vertical mixing after assimilation of localized urban measurements may result from both the increased surface heating and the large surface roughness imposed by the urban environment (Piringer et al., 2007). These findings highlight the fact that the observational nudging approach might be an efficient solution for model deficiencies in complex terrains such as the urban environment. In fact, the nudging approach not only adjusted the meteorological variables, but also allowed a better description of the urban PBL structure which strongly impacted the dispersion simulations by HYSPLIT.

As previously mentioned, the dispersion simulations presented in this study were hypothetical releases, which means that real pollutant dispersions were unknown. Because tracer experiments to evaluate HYSPLIT simulations were not available for the studied time periods, and to evaluate existing non-UrbanNet capabilities, HYSPLIT was driven by nudged WRF using meteorological datasets collected from the DCA and IAD airports. The results demonstrated that the use of the data from the DCA airport, which is located closer to the downtown area, to nudge WRF model provided HYSPLIT simulations very similar to the ones using HCHB data. This provides strong evidence that local data are essential to improve the accuracy of dispersion modeling.

As a recent addition to the UrbanNet measurement program, LIDAR systems have been collocated with exiting tower stations in central Washington, D.C. Data now being collected provide an opportunity to combine tower and LIDAR data to better describe the vertical wind profile in order to improve the performance of NWP models and the HYSPLIT model in simulating the transport and mixing of pollutants in the NCR. Furthermore, we are planning to implement an urban canopy model in WRF to consider the heterogeneity of the urban structure. This implementation will help us understand and model the structure of the urban boundary layer where most of the world's population live and work.

Acknowledgements

We gratefully acknowledge Mr. Bruce Hicks of MetCorps for his comments and suggestions which greatly helped us to improve the paper. This work was supported by NOAA Cooperative Institutes, Award NA19NES4320002, at the Cooperative Institute for Satellite Earth System Studies, University of Maryland.

References

Abida, R., Addad, Y., Francis, D., Temimi, M., Nelli, N., Fonseca, R., Nesterov, O., and E. Bosc, E., 2022. Evaluation of the Performance of the WRF Model in a Hyper-Arid Environment: A Sensitivity Study. Atmosphere, 13, 985. https://doi.org/10.3390/atmos13060985.

Baklanov, A., Grimmond, C.S.B., Carlson, D., Terblanche, D., Tang, X., Bouchet, V., Lee, B., Langendijk, G., Kolli, R.K., Hovsepyan, A., 2018. From urban meteorology, climate and environment research to integrated city services. Urban Clim. 23, 330–341. https://doi.org/10.1016/j.uclim.2017.05.004.

Barlow, J.F., 2014. Progress in observing and modelling the urban boundary layer. Urban Climate 10, 216-240. https://doi.org/10.1016/j.uclim.2014.03.011.

Benjamin, S. G., Brown, J. M., Brunet, G., Lynch, P., Saito, K., and Schlatter, T. W., 2019. 100 years of progress in forecasting and NWP applications. A Century of Progress in Atmospheric and Related Sciences: Celebrating the American Meteorological Society Centennial, Meteor. Monogr., No. 59, Amer. Meteor. Soc., https://doi.org/10.1175/AMSMONOGRAPHSD-18-0020.1.

Branch, O., Schwitalla, T., Temimi, M., Fonseca, R., Nelli, N., Weston, M., Milovac, J., and Wulfmeyer, V., 2021. Seasonal and diurnal performance of daily forecasts with WRF V3.8.1 over the United Arab Emirates. *Geosci. Model Dev.*, **14**, 1614-1637. https://doi.org/10.5194/gmd-14-1615-2021.

Britter, R.E., Hanna, S.R., 2003. Flow and dispersion in urban areas. Annu. Rev. Fluid Mech. 35, 469–496. https://doi.org/10.1146/annurev.fluid.35.101101.161147.

Chen, F., and Dudhia, J., 2001. Coupling an Advanced Land Surface–Hydrology Model with the Penn State–NCAR MM5 Modeling System. Part I: Model Implementation and Sensitivity. *Mon. Wea. Rev.*, **129**, 5 69–585, https://doi.org/10.1175/1520-0493(2001)129<0569:CAALSH>2.0.CO;2

Chen, J., Yang, Y., and Tang, J., 2022. Bias correction of surface air temperature and precipitation in CORDEX East Asia simulation: What should we do when applying bias correction? *Atmospheric Research*, **280**, 106439, https://doi.org/10.1016/j.atmosres.2022.106439.

Chai, T., Draxler, R., and Stein, A., 2015. Source term estimation using air concentration measurements and a Lagrangian dispersion model e Experiments with pseudo and real cesium-137 observations from the Fukushima nuclear accident. *Atmospheric Environment*, **106**, 241-251, https://doi.org/10.1016/j.atmosenv.2015.01.070.

Cuchiara, G. C., and Rappengluck, B., 2019: Simulating the influence of convective decay parameterization for a case study in Houston, TX. *Atmospheric Environment*, **204**, 68-77, https://doi.org/10.1016/j.atmosenv.2019.02.016.

Deng, A., Stauffer, D., Gaudet, B., Dudhia, J., Hacker, J., Bruyere, C., Wu, W., Vandenberghe, F., Liu, Y., Bourgeois, A. Update on WRF-ARW end-to-end multi-scale FDDA system. In Proceedings of the 10th WRF Users' Workshop, Boulder, CO, USA, 23–26 June 2009; NCAR: Boulder, CO, USA, 2009.

Draxler, R.R., and Hess, G. D., 1997. Description of the HYSPLIT_4 modeling system. NOAA Tech.

Memo. ERL ARL-224, 24 pp.

Draxler, R.R., and Hess, G. D., 1998. An overview of the HYSPLIT_4 modeling system for trajectories, dispersion, and deposition. Aust. Meteor. Mag., 47, 295–308.

Fenger, J., 1999: Urban air quality. Atmospheric Environment, 33, 4877-4900.

Grimmond, C. S. B., and Oke, T. R., 1999: Heat Storage in Urban Areas: Local-Scale Observations and Evaluation of a Simple Model. J. Appl. Meteor. Climatol., 38, 922–bv940, https://doi.org/10.1175/1520-0450(1999)038<0922:HSIUAL>2.0.CO;2.

Haupt, S.E., Hanna, S., Askelson, M., Shepherd, M., Fragomeni, M.A., Debbage, N., Johnson, B., 2019. 100 years of Progress in applied meteorology. Part II: applications that address growing populations. Meteorol.Monogr. 59, 23.1-23.40. https://doi.org/10.1175/AMSMONOGRAPHS-D-18-0007.1.

Hegarty, J., Draxler, R.R., Stein, A.F., Brioude, J., Mountain, M., Eluszkiewicz, J., Nehrkorn, T., Ngan, F., Andrews, A., 2013: Evaluation of Lagrangian particle dispersion models with measurements from controlled tracer releases. J. Appl. Meteor. Climatol., 52, 2623– 2637, https://doi.org/10.1175/JAMC-D-13-0125.1.

Hicks, B.B., 2005. Urban dispersion for the 21st century. WIT Transactions on The Built Environment, 82: 555-566.

Hicks, B. B., Callahan, W. J., Pendergrass III, W. R., Dobosy, R. J. and Novakovskaia, E. 2012: Urban turbulence in space and time. J. Appl. Meteor. Climatol., **51**, 205–218.

Hicks, B.B., Novakovskaia, E., Dobosy III, R.J., Callahan, W.J., 2013. Temporal and spatial aspects of velocity variance in the urban surface roughness layer. J. Appl. Meteorol. Climatol. 52, 668–681. https://doi.org/10.1175/JAMC-D-11-0266.1.

Jia, M. W., X. Huang, K. Ding, Q. Liu, D.R. Zhou, A.J. Ding, 2021: Impact of data assimilation and aerosol radiation interaction on Lagrangian particle dispersion modelling. Atmos. Environ., 247, 118179, https://doi.org/10.1016/j.atmosenv.2020.118179.

Kelly, F.J., Fussell, J.C., 2015: Air pollution and public health: emerging hazards and improved understanding of risk. *Environ. Geochem. Hlth.*, **37,** 631-649, https://doi.org/10.1007/s10653-015-9720-1.

Leelőssy, A., Molnár, F., Izsák, F., Havasi, Á., Lagzi, I., and Mészáros, R., 2014. Dispersion modeling of air pollutants in the atmosphere: a review" *Open Geosciences*, vol. 6, no. 3, 2014, pp. 257-278. https://doi.org/10.2478/s13533-012-0188-6.

Lichiheb, N., Hicks, B.B, Myles, L., 2023. An evaluation of meteorological data prediction over Washington, D.C.: Comparison of DCNet observations and NAM outputs. Urban climate, 48, 101410. https://doi.org/10.1016/j.uclim.2023.101410.

National Centers for Environmental Prediction/National Weather Service/NOAA/U.S. Department of Commerce. 2015, updated daily. NCEP GDAS/FNL 0.25 Degree Global Tropospheric Analyses and Forecast Grids. Research Data Archive at the National Center for Atmospheric Research, Computational and Information Systems Laboratory. Accessed 29 March, 2022, https://doi.org/10.5065/D65Q4T4Z.

Ngan, F., Loughner, C. P. and Stein, A. F., 2019: The evaluation of mixing methods in HYSPLIT using measurements from controlled tracer experiments. Atmos. Environ., 219, 117043.

Ngan, F., Stein, A. and Draxler, R., 2015 a. Inline Coupling of WRF–HYSPLIT: Model Development and Evaluation Using Tracer Experiments. J. Appl. Meteor. Climatol., 54,1162–1176.

Ngan, F., Cohen, M., Luke, W., Ren, X., Draxler, R., 2015 b. Meteorological modeling using the WRF-ARW model for Grand Bay intensive studies of atmospheric mercury. Atmosphere 6, 209–233. https://doi.org/10.3390/atmos6030209.

Ngan, F., Loughner, C.P., Zinn, S., Cohen, M., Lee, T.R., Dumas, E., Schuyler, T.J., Baker, B., Maloney, J., Hotz, D., and Mathews, G., 2023. The use of small uncrewed aircraft system observations in meteorological and dispersion modeling. J. Appl. Meteor. Climatol., 62, 817-834. https://doi.org/10.1175/JAMC-D-22-0182.1.

Onodera, N., Idomura, Y., Hasegawa, Y. Nakayama, H., Shimokawabe, T., and Aoki, T., 2021. Real-Time Tracer Dispersion Simulations in Oklahoma City Using the Locally Mesh-Refined Lattice Boltzmann Method. *Boundary-Layer Meteorol* **179**, 187–208. https://doi.org/10.1007/s10546-020-00594-x.

Pataki, D.E., Xu, T., Luo, Y.Q., Ehleringer, J.R., 2007. Inferring biogenic and anthropogenic carbon dioxide sources across an urban to rural gradient. *Oecologia*, **152**, 307-322, https://doi.org/10.1007/s00442-006-0656-0 .

Pendergrass, W., Nichiheb, N. White, R., Hicks, B.B. and Myles, L., 2020: High-Resolution Meteorological Monitoring over the National Capital Region: Data from the DCNet Network at the US Department of Commerce Herbert C. Hoover Building Station. NOAA Tech Memo OAR ARL-280. 59 pp.

Piersante, J. O., Schumacher, R. S. and Rasmussen, K. L. 2021. Comparison of Biases in Warm-Season WRF Forecasts in North and South America. *Weather and Forecasting*, **36**, 979-1001, https://doi.org/10.1175/WAF-D-20-0062.1.

Piringer, M., Joffre, S., Baklanov, A. Christen, A., Deserti, M., De Ridder, K., Emeis, S., Mestayer, P., Tombrou, M., Middleton, D., Baumann-Stanzer, K., Dandou, A., Karppinen, A., and Burzynski, J., 2007. The surface energy balance and the mixing height in urban areas—activities and recommendations of COST-Action 715. Boundary-Layer Meteorol 124, 3–24. https://doi.org/10.1007/s10546-007-9170-0.

Powers, J.G., Klemp, J.B., Skamarock, W.C., Davis, C.A., Dudhia, J., Gill, D.O., Coen, J.L., Gochis, D.J., Ahmadov, R., Peckham, S.E., Grell, G.A., Michalakes, J., Trahan, S., Benjamin, S.G., Alexander, C.R., Dimego, G.J., Wang, W., Schwartz, C.S., Romine, G.S., Liu, Z., Snyder, C., Chen, F., Barlage, M.J., Yu, W., and Duda, M.G., 2017. The weather research and forecasting model: overview, system efforts, and future directions. Bull. Am. Meteorol. Soc. 98 (8), 1717–1737. https://doi.org/10.1175/BAMS-D-15-00308.1.

Rudd, A., Robins, A. G., Lepley, J. J. and Belcher, S., 2012. An inverse method for determining source characteristics for emergency response applications. Boundary-Layer Meteorology. 144, 1-20. https://doi.org/10.1007/s10546-012-9712-y

Stein, A.F., Draxler, R.R., Rolph, G.D., Stunder, B.J.B., Cohen, M.D., Ngan, F., 2015. NOAA's HYSPLIT atmospheric transport and dispersion modeling system. Bull. Am. Meteorol. Soc. 96, 2059–2077.

Tomasi, E. L., Giovannini, M., Falocchi, G., Antonacci, P.A., Jimenez, B., KOsovic, S., Alessandrini, D., Zardi, L., Delle Monache, E., Ferrero, 2019: Turbulence parameterizations for dispersion in sub-kilometer horizontally non-homogeneous flows. Atmospheric Research, 228, 122 – 136, https://doi.org/10.1016/j.atmosres.2019.05.018.